Available online at www.sciencedirect.com
ScienceDirect
Applied Surface Science 254 (2007) 781–784
applied surface science
www.elsevier.com/locate/apsusc

Design and spectroscopic reflectometry characterization of pulsed laser deposition combinatorial libraries

Peter K. Schenck [a,*], Nabil D. Bassim [a], Makoto Otani [a], Hiroyuki Oguchi [b], Martin L. Green [a]

[a] Ceramics Division, National Institute of Standards and Technology, Gaithersburg, MD 20899, USA
[b] Department of Materials Science and Engineering, University of Maryland, College Park, MD 20742, USA

Received 13 February 2007; accepted 29 May 2007
Available online 10 July 2007

Abstract

The goal of the design of pulsed laser deposition (PLD) combinatorial library films is to optimize the compositional coverage of the films while maintaining a uniform thickness. The deposition pattern of excimer laser PLD films can be modeled with a bimodal $\cos^n$ distribution. Deposited films were characterized using a spectroscopic reflectometer (250–1000 nm) to map the thickness of both single composition calibration films and combinatorial library films. These distribution functions were used to simulate the composition and thickness of multiple target combinatorial library films. The simulations were correlated with electron-probe microanalysis wavelength-dispersive spectroscopy (EPMA-WDS) composition maps. The composition and thickness of the library films can be fine-tuned by adjusting the laser spot size, fluence, background gas pressure, target geometry and other processing parameters which affect the deposition pattern. Results from compositionally graded combinatorial library films of the ternary system Al_2O_3–HfO_2–Y_2O_3 are discussed.

PACS : 81.15Fg

Keywords: Combinatorial; Thin films; Reflectometry

1. Introduction

The use of combinatorial techniques for optimization of film properties and discovery of new materials with novel properties for use in thin film devices [1,2] requires the development of rapid throughput measurement techniques to characterize the library films. This paper describes the use of high throughput spectroscopic reflectometry to determine the deposition patterns from both single composition calibration films and multi-composition library films, produced in a commercial combinatorial PLD tool [3]. The PLD tool utilizes a multiple target system combined with an indexed rotating substrate holder/heater to produce binary or ternary library films by the natural spread technique. The procedure to create a ternary library film consists of depositing a sub-monolayer from the first target at 0°, rotating the substrate to 120°, depositing a sub-monolayer from target two, rotating the substrate to 240° and depositing a sub-monolayer from the third target. This cycle is repeated a sufficient number of times to produce the desired film thickness. The ternary system Al_2O_3–HfO_2–Y_2O_3, potentially useful as high-k dielectrics [4], was used as a test case in this paper.

2. Experimental

2.1. Calibration procedure

The preparation of the library fabrication recipe for the PLD tool, i.e. number of laser pulses per cycle for each target and number of cycles, requires calibration runs for each of the targets, under the planned deposition conditions (pressure, laser fluence, temperature, etc.). The thickness profiles of these calibration films are mapped using a spectroscopic reflectometer [5]. Single composition calibration films were made from each of the HfO_2, Al_2O_3, and Y_2O_3 targets with a KrF excimer laser focused to a fluence of ~15 J/cm^2. Each film was deposited with 10,000 laser pulses, to produce a film of

* Corresponding author. Tel.: +1 301 975 5758; fax: +1 301 975 5334.
E-mail address: pkschenck@nist.gov (P.K. Schenck).

0169-4332/$ – see front matter
doi:10.1016/j.apsusc.2007.05.086

appropriate thickness. The target to substrate distance was 6.5 cm, and the substrate temperature was 400 °C. The calibrations were made at two oxygen pressures 1.33 Pa and 13.3 Pa.

The production of a ternary library film uses substrate rotations of 0°, 120°, and 240° for each target, during each cycle of the deposition recipe. The calibration films were deposited with these rotations so that the results could be used to directly design and predict the library films. The reflection spectra from the calibration films were mapped radially (r,θ) from $r = 0$ mm to 38 mm, with an angular spacing ($\Delta\theta$) designed to give approximately a 1 mm × 1 mm grid. The spatial resolution, or spot size, of the reflectometer was 0.2 mm. On a 76.2 mm wafer, 4460 points were mapped. The analysis of the spectroscopic reflectometer data assumed textbook values [6] for the index of refraction of the films. The results for a typical calibration run are shown in Fig. 1. There are some areas of the calibration film where no thickness value was determined by the fitting algorithm which assumes simple thin film interference [7]. There are also edge effects apparent in Fig. 1 to the right of the center, where steep thickness gradients are observed. In order to design and predict the library film over the whole substrate a deposition model was used, as discussed in the next section.

2.2. Deposition distribution model for library films

The focused spot of the PLD excimer laser is a rectangle, resulting in a different spread of the plume in the directions normal to the long axis of the laser spot (here the X-axis) and parallel to the long axis of the laser spot (here the Y-axis). The resulting thickness map, for each target, is fit to a bimodal $\cos^n$ distribution function [8] of the form:

$$T(x,y) = T_0 \cos^m \theta_x \cos^n \theta_y \tag{1}$$

where T_0 is the thickness at the center of the deposition pattern, θ_x and θ_y are the angles, in the x and y direction, of the divergence of the material plume from the centerline of the target, and m and n are the exponential rates of decrease in the thickness of the film in the x and y directions. The angle of divergence, θ_x, as a function of x, is given by

$$\theta_x = \arctan\left(\frac{x - x_0}{z}\right) \tag{2}$$

where z is the distance between the substrate and the target and x_0 is the x coordinate of the center of the deposition pattern, normally the center of the PLD plume. The value of $\cos^m(\theta_x)$ may then be expressed as

$$\cos^m \theta_x = \left(\frac{z}{\sqrt{z^2 + (x - x_0)^2}}\right)^m \tag{3}$$

for the x direction, and as

$$\cos^n \theta_y = \left(\frac{z}{\sqrt{z^2 + (y - y_0)^2}}\right)^n \tag{4}$$

for the y-direction, where y_0 is the y coordinate of the center of the deposition pattern (PLD plume).

In a ternary library film equation (1) is determined for each of the three targets. In general all of the fit parameters (T_0, m, n, x_0, and y_0) are different for each target and deposition condition. Eq. (1) can be used to predict the compositional coverage by conversion to a molar fraction by multiplying $T(x,y)$ by the density of the material and dividing by the molecular weight. In this work the design goal was to have a recipe where the per cycle deposition was less than a monolayer, the total thickness on axis at Y_2O_3 was nominally 100 nm, and the nominal atomic ratios were roughly equal in the center of the film to aid in the EPMA-WDS determination of the composition map. Once the recipe was determined, the three deposition rate equations were used to simulate the library film deposition and determine the predicted compositional coverage of the library film.

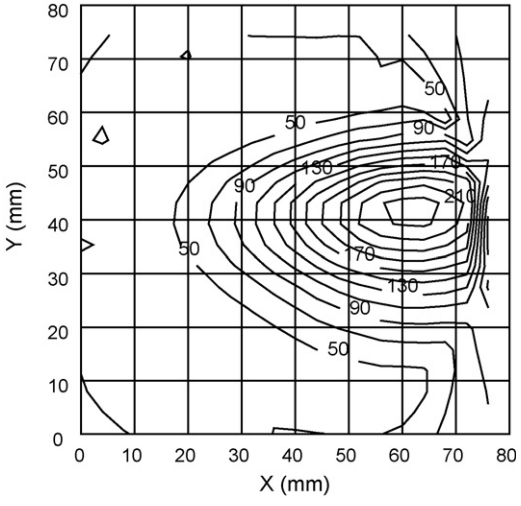

Fig. 1. Calibration data for an HfO_2 film grown with 1.33 Pa O_2 background pressure. Thickness contours are in nm.

2.3. EPMA-WDS determination of the composition

The compositions of the library films were determined by electron-probe microanalysis with wavelength-dispersive spectroscopy (EPMA-WDS). The substrates were cut in half to fit the EPMA-WDS sample holder, which also accommodated reference materials. Measurements were performed on an X–Y grid at 2 mm intervals. Compositions were calculated by comparison with X-ray fluorescence peak areas of the library film and reference materials. The reported accuracy of the individual atomic fractions is approximately 1% when using in situ standards.

3. Results and discussion

3.1. Simulation of the library films: the role of alignment

In the original design of the commercial PLD tool, the laser spot on the target is along the centerline of the substrate and deposition chamber. The analysis of calibration films determined that the values of the center of the distributions (x_0,y_0)

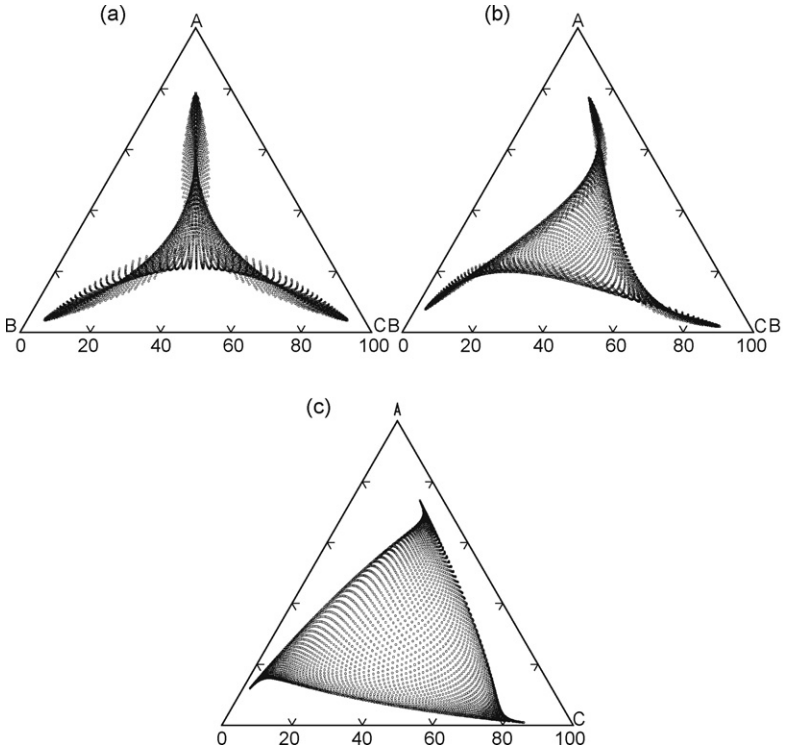

Fig. 2. Simulation of ternary coverage from three targets with $m = 6$ and $n = 17$ with y-offsets from center of (a) 0 mm, (b) 6 mm, and (c) 12 mm.

were not exactly along the centerline of the substrate. These offsets were added to the simulations of the deposition pattern and compositional coverage. Increasing the deviations from the design alignment, particularly in the y direction (perpendicular to the centerline of the wafer and plane of the laser), predicted more thickness uniformity and better compositional coverage. Fig. 2 illustrates that a small offset from the centerline can dramatically affect the compositional coverage of the natural spread technique for PLD combinatorial library films.

3.2. Simulation of the library films: thickness and compositional coverage

The results from the six calibrations are presented in Table 1. The bimodal cosine model was fit to data from the calibration films running from the center of the wafer to approximately the center of the deposition pattern in order to remove edge effects. These results were used to design the recipes for the two library films. The result of the higher oxygen pressure was to reduce the deposition rate and spread the plume out in space, i.e. lower values of m and n, due to scattering of the plume species by the higher density of gas molecules. These results are consistent with Monte Carlo calculations of the plume expansion [9]. The simulation results for the $HfAlYO_x$ films produced at oxygen pressures of 1.33 Pa and 13.3 Pa are shown in Fig. 3a and b, respectively. The simulation at higher pressure, with more symmetric values of m and n, predicts better coverage of the ternary system.

3.3. Comparison of the simulation with EMPA-WDS composition mapping

Fig. 4a and b shows the ternary coverage determined by EMPA-WDS for the 1.33 Pa and 13.3 Pa O_2 films, respectively. Although not shown, the individual cation EMPA-WDS maps are very similar to the cation simulation maps generated with the bimodal $\cos^n$ deposition model using the calibration values from Table 1 and the recipe derived from them. The main difference is that edge effects are apparent in the maps. The result is that the bimodal $\cos^n$ model is most accurate from the center of the

Table 1
Results of fitting equations (1)–(4) to the calibration film data

Sample no.	Target material	Oxygen pressure (Pa)	T_0 (nm) thickness at center	x_0-coordinate at center	y_0-coordinate at center	m cosine distribution in x-direction	n cosine distribution in y-direction
1	HfO_2	1.33	256	64.0	39.6	7.75	29.0
2	HfO_2	13.3	190	61.0	38.8	9.0	18.4
3	Al_2O_3	1.3	258	57.0	49.0	5.7	11.6
4	Al_2O_3	13.3	184	52.8	46.3	7.6	9.65
5	Y_2O_3	1.3	327	62.0	45.4	6.5	18.1
6	Y_2O_3	13.3	250	59.0	45.0	8.0	12.5

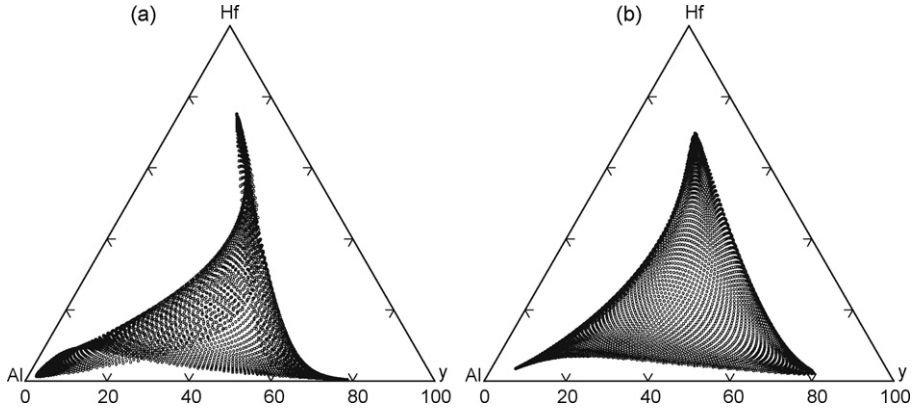

Fig. 3. Simulation of $HfAlYO_x$ film using the calibration values from Table 1 for (a) 1.33 Pa O_2 growth and (b) 13.3 Pa O_2 growth.

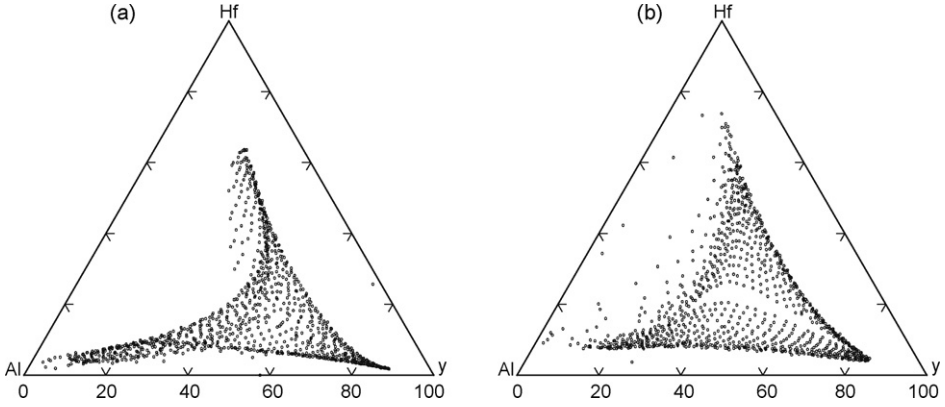

Fig. 4. EPMA-WDS results of the ternary $HfAlYO_x$ library films for (a) 1.33 Pa O_2 growth and (b) 13.3 Pa O_2 growth. The "hole" in (b) is an artifact due to cleaving the wafer to fit in the EPMA-WDS holder.

deposition pattern towards the center of the substrate. Accordingly the model is only applied to the data within a radius, from the center of the wafer, to the center of the deposition pattern.

To obtain a meaningful evaluation of the simulation to the EMPA-WDS data, the coefficient of determination, or correlation factor [10], is calculated for each cation's EMPA-WDS map and simulation map. Only the central (13–63 mm in x and y) data and simulation are used to calculate r^2. The average of r^2 derived from the three cations is used as a figure of merit for the simulation. The EMPA-WDS maps, and the simulations based on the calibration, have differences because the data, taken on different apparati, have different coordinate systems. There is both an XY offset and rotational offset of the reference frames. The value of r^2 was calculated for several X, Y, and rotational offsets. The result is a series of contour plots of r^2 versus X and Y for each angular offset. When the EMPA-WDS data is rotated 5° and shifted by +2 mm in X and −3 mm in Y to align the respective reference frames, a correlation of $r^2 = 0.98$ is obtained.

4. Conclusions

It has been demonstrated that using a simple bimodal cosine power distribution function for the PLD deposition rate from three targets, the composition and thickness of ternary library films can be predicted, and agree, within measurement resolution, with experimental EMPA-WDS results. Thus, we can have a high degree of confidence that the modeling design of experiments will yield the predicted thickness and compositional coverage, making the combinatorial PLD tool very useful for routine library design. Costly experimental verification may be avoided for many applications.

Acknowledgements

The authors would like to thank K.-S. Chang, E.J. Heilweil, and A.J. Paul of NIST for helpful suggestions and discussions.

References

[1] J.J. Hanak, J. Mater. Sci. 5 (1970) 964.
[2] X.D. Xiang, X. Sun, G. Briceno, Y. Lou, K.-A. Wang, H. Chang, W.G. Wallace-Freedman, S.-W. Chen, P.G. Schultz, Science 268 (1995) 1738.
[3] H.M. Christen, S.D. Silliman, K.S. Harshavardhan, Rev. Sci. Inst. 72 (2001) 2673.
[4] G.D. Wilk, R.M. Wallace, J.M. Anthony, J. Appl. Phys. 89 (2001) 5243.
[5] P.K. Schenck, D.K. Kaiser, A.V. Davydov, Appl. Surf. Sci. 223 (2004) 200.
[6] E.D. Palik, Handbook of Optical Constants of Solids, Academic Press, San Diego, 1998.
[7] O.S. Heavens, Optical Properties of Thin Solid Films, Dover, New York, 1991.
[8] K.L. Saenger, in: D.B. Chrisey, G.K. Hubler (Eds.), Pulsed Laser Deposition of Thin Films, Wiley/Interscience, 1994, p. 199.
[9] P.K. Schenck, J.W. Hastie, A.J. Paul, D.W. Bonnell, Opt. Eng. 35 (1996) 3199.
[10] H.D. Young, Statistical Treatment of Experimental Data, McGraw-Hill, New York, 1962.